

SUPPLEMENT

Validation of N95 filtering facepiece respirator decontamination methods available at a large university hospital

Krista R. Wigginton¹, Peter J. Arts¹, Herek Clack¹, William J Fitzsimmons², Mirko Gamba³, Katherine R. Harrison¹, William LeBar⁴, Adam S. Lauring², Lucinda Li¹, William W. Roberts^{5,6}, Nicole Rockey¹, Jania Torreblanca⁴, Carol Young⁴, Loïc G. Anderegg^{7,8}, Amy M. Cohn⁹, John M. Doyle^{7,8}, Cole M. Meisenhelder⁷, Lutgarde Raskin¹, Nancy G. Love^{1*}, Keith S. Kaye^{2*}

Affiliations

¹*Department of Civil & Environmental Engineering, University of Michigan, Ann Arbor, MI, USA* ; ²*Division of Infectious Diseases, Department of Internal Medicine, University of Michigan Health System, Ann Arbor, MI, USA*; ³*Department of Aerospace Engineering, University of Michigan, Ann Arbor, MI, USA*; ⁴*Department of Pathology, Clinical Microbiology, University of Michigan Health System, Ann Arbor, MI, USA*; ⁵*Department of Urology, University of Michigan Health System, Ann Arbor, MI, USA*; ⁶*Department of Biomedical Engineering, University of Michigan, Ann Arbor, MI, USA*; ⁷*Department of Physics, Harvard University, Cambridge, MA, USA*; ⁸*Harvard-MIT Center for Ultracold Atoms, Cambridge, MA USA*; ⁹*Department of Industrial & Operations Engineering, University of Michigan, Ann Arbor, MI, USA*

Filtration Performance Testing.

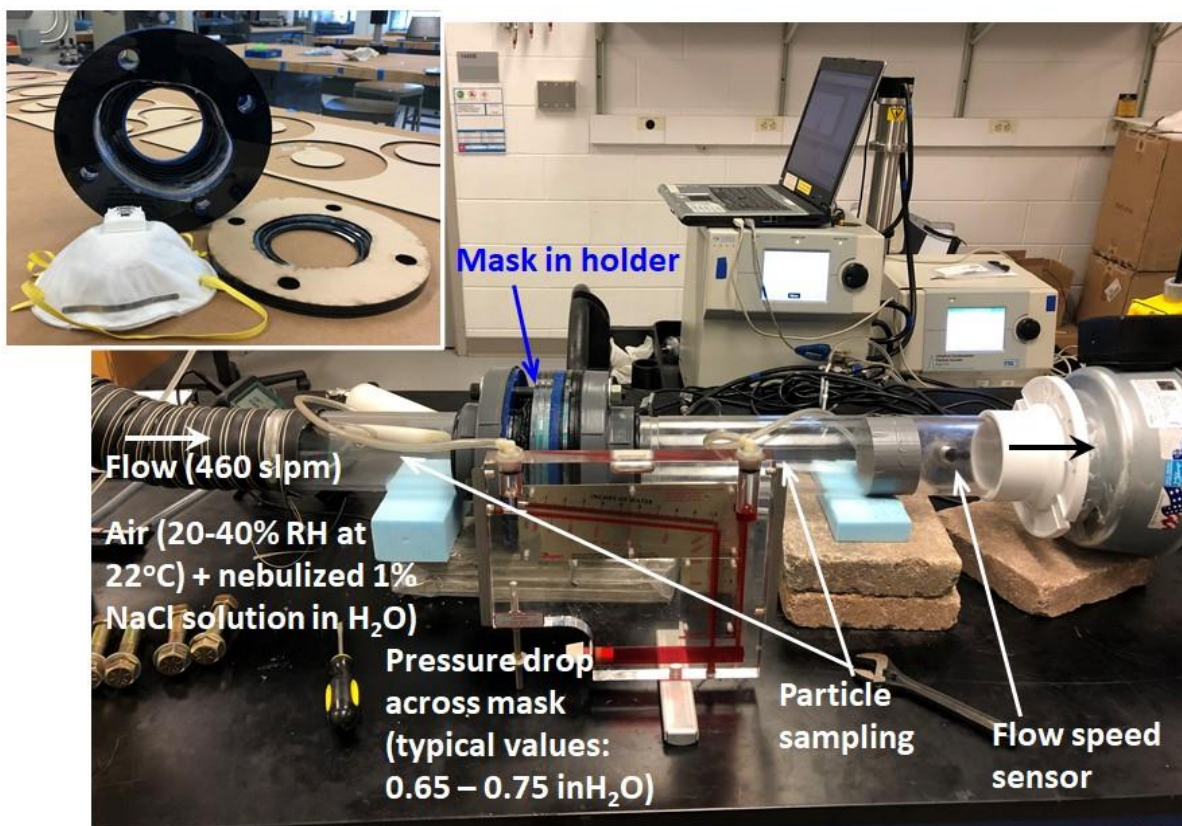
The experimental apparatus is shown in Figure e1 with the exception of the droplet generator and droplet drying column. A consumer-grade medical nebulizer (Okasiman OKA-517) produced fine aqueous mists at either 1 or 0.6 mL/min from 15 mL of 1% (by mass) NaCl in aqueous solution. The mist was drawn with unfiltered ambient air (nominally 22 °C 20-40% relative humidity (RH)) into a flexible hose that acted as a droplet drying column (8.9 cm ID x 4 m L) by the controlled induced draft (ID) airflow (nominally 460 L/min with supplemental confirmation tests at 92 L/min) generated by an ID fan at the exhaust of the apparatus. Although HEPA filtered air is usually used for aerosol studies, separate measurements of the particle number concentration (#/cc) in the ambient laboratory air indicated generally two to four orders of magnitude lower number concentrations of particles in the ambient air than the generated droplets and particles at all test conditions. The drying column connects to one of two Plexiglas tubes (8.9 cm OD x 7.6 cm ID x 30 cm L) that insert into the upstream and downstream faces of the custom fixture into which each mask is mounted during testing. Both tubes were drilled and tapped to allow upstream and downstream sampling of the flow from the tube wall. Supplemental testing showed that wall sampling yielded 20% lower particle concentration measurements than when sampling through an extractive probe near the flow centerline, however this bias is eliminated by examining upstream/downstream ratios of measured particle concentrations. The custom mask-mounting fixture consists of multiple Plexiglas rings (17.5 cm OD x 6.35 mm thickness), processed using a laser cutter to produce IDs that progressively increase and morph from a uniform circular cross-section of 8.9 cm to a quasi-oval cross-section customized to match the outlines of the various masks tested. Four bolts hold the entire fixture in compression with each mask pressed between two rubber gaskets and in an upstream-facing orientation. The downstream Plexiglas tube has an additional port through which centerline air velocity was measured using a hot-wire anemometer probe (Extech model 407123) downstream of each mask. A variable speed ID fan and additional temperature and RH measurement downstream of the anemometer complete the apparatus.

Upstream and downstream of each mask, extractive sampling from the flow, in triplicate, provided particle size distributions and particle concentrations (#/cc). Continuously extracted samples underwent narrow band pass size selection, followed by particle counting. A TSI 3936 Scanning Mobility Particle Sizer (SMPS) includes a TSI series 3080 Electrostatic Classifier with a Differential Mobility Analyzer (DMA) which together admit only particles within predefined size range bands between 11 and 489 nm to pass while all others are removed. The size classified particles then enter a series 3776 Condensation Particle Counter (CPC) for measurement of particle concentration. A PC running the TSI Aerosol Instrument Manager software collected and managed the sampled data. Table e2 presents a summary of the experimental conditions.

The nominal particle size distributions produced after drying of the saline droplets generated by the nebulizer in the present experiments reflect the influences of multiple experimental constraints including initial air temperature and RH, air flow rate, nebulization rate, drying column length and the size and distribution of droplets generated by the nebulizer. Although the count mean diameter is larger than that called for in the ASTM standard, the overall distribution still comprises particles down to ~ 11 nm, for which upstream/downstream comparisons can yield size-specific penetration fractions for a given mask and allow inter-comparison between different masks.

All of the foregoing particle penetration results were collected at a nominal airflow velocity of 168 cm/s, corresponding to a nominal volumetric flow rate of 460 L/min which is higher than the ASTM testing specification of 85 L/min. Subsequent testing confirmed the findings of previous researchers (1) that under constant air flows, N95 mask particulate penetration rates increased with increasing volumetric airflow rate (data not shown). To the extent that particle penetration rates measured at 460 L/min do not approach the 5% required of N95 masks, the inference is that their ASTM-traceable performance would be lower, i.e., high-flow-rate penetration performance can be considered overly conservative in comparison to the performance expected at the ASTM standard conditions. The vast majority of new, unused and unused but sterilized N95 masks tested here fall into this category: high-flow-rate particle penetration performance met the N95 standard, implying that such masks would also meet the standard at the ASTM-traceable flow rate of 85 L/min.

One type of mask tested did not produce performance, at the higher airflow rate of 460 L/min, that would meet the N95 certification standard, a Chinese-manufactured KN95 mask (LJK). This brand of KN95 mask yielded overall particle penetration rates exceeding 40% at airflow rates of 460 L/min. When retested at 85 L/min, the corresponding overall particle penetration rate dropped to 21%, which still far exceeds the N95 certification standard.



eFigure 1. Particle filtration testing experimental apparatus. Droplet-generating nebulizer and drying column not shown. Inset: Image of custom-built mask holder comprised of layers of laser-cut Plexiglas disks that transition the flow from circular cross-section to the quasi-oval cross-sections of each model of N95 mask.

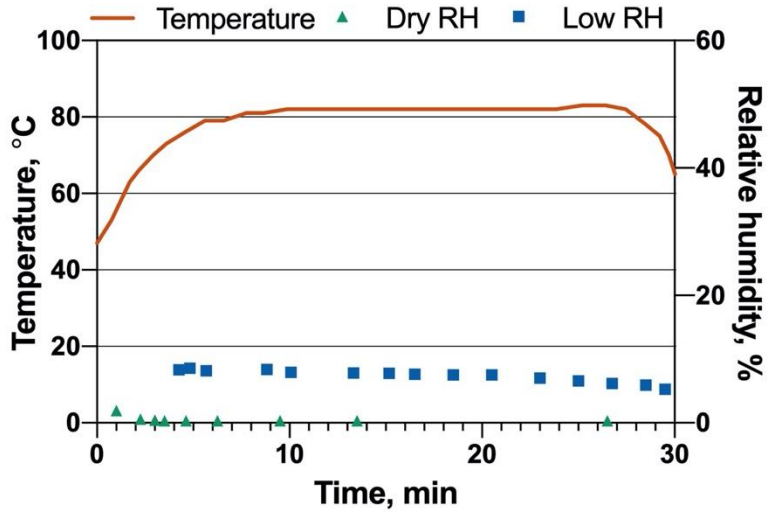
eTable 1. Filtration Performance of Various FFRs after Decontamination Treatment.

Decontamination treatment by FFR brand/model	Minimum filtration efficiency (# of treatment cycles ^a)	Filtration stability index ^b	Pressure drop (mm H ₂ O)	Fit test outcome # passed after (#) cycles
UV-PX + dry heat				
• 3M 8511	>97.5% (5)	0.14	17.5	nt
• 3M 8210	>97.5% (10)	0.19	17.5	nt
UV-PX + low RH heat				
• 3M 8210c	>97.5% (5)	0.08	17.5	3/3 (5), 1/1 (10)
• Moldex 1511	>98.5% (10)	0.07	17.5	3(5)
UV-PX + low RH heat + VHP				
• 3M 8210c	>97.5 (5, 5) ^h	0.08	17.5	nt
HPGP				
• 3M 8210	>58% (5)	7.9	17.5	nt
EtO				
• 3M 8210	>99%	0.3	17.5	nt
VHP				
• 3M 8210	>99% (10)	0.08	17.5	7 (1) ^g
• Moldex 1511	>99% (10)	0.06	17.5	1 (1) ^g
UV-PX + dry heat + VHP				
• 3M 8210	>97.5% (10, 4) ^h	0.3	17.5	nt
None/No Treatment ^f				
• LKJ KN95	>79% (N/A)	N/A		nt
• Winner KN95	>99% (N/A)	N/A		nt
• Bi Wei Kang KN95	>99% (N/A)	N/A		nt
• Zhenshanmei KN95	>95% (N/A)	N/A		nt

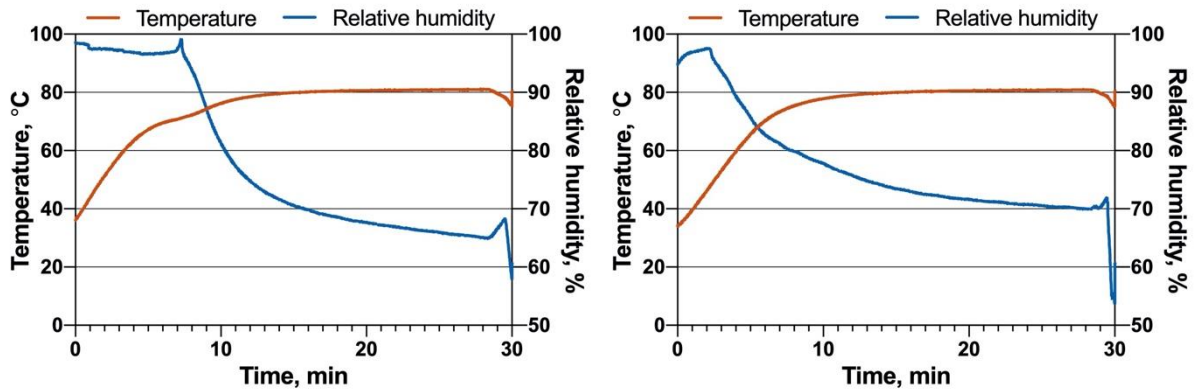
nt=not tested. ^aSingle cycle duration values, by treatment method: Dry or low RH heat, 30 min.; UV-PX, 5 min; VHP using Condition 2; EtO, 15 hrs. ^bFiltration stability index is defined as the ratio of the range of measured filtration efficiency values to the maximum number of treatment cycles for a specified decontamination method. Smaller index values represent less impact of decontamination on filtration performance. ^cMasks uncontained during treatment; moisture added to treatment environment. ^dMasks held in individual containers; moisture added to containers. ^eTwo masks treated for 4 and 8 hours are considered as having undergone 1 and 2 four-hour cycles, respectively. ^fAll KN95 results obtained at an air flow rate of 85 L/min. ^gtesting with VHP continues; table will be updated when results are available. ^hMasks first treated with UV+heat and subsequently treated with VHP show the number of cycles for each process, respectively.

eTable 2. Experimental conditions for particle filtration testing.

Air, volumetric flow rate [L/min]	460 (with limited data at 85)
Air, ambient temperature [°C]	22 (nominal)
Air, ambient RH [%]	20-40
Aerosol generation rate [mL/min]	1 (with limited data at 0.6)
Aerosol size distribution parameters (nominal)	



eFigure 2. Temperature and relative humidity (RH) profile during the dry cycle of the hospital instrument washer, set at 82 °C for 30-minute cycle. The dry RH run was operated with no effort to modify humidity. The low RH run was supplemented with seven 43 cm x 66 cm surgical towels receiving 700 mL deionized water to enhance RH beyond baseline. The temperature profile was taken during the low RH run and is typical of dry RH runs.



eFigures 3. Temperature and humidity profiles from two runs during a dry cycle in the same hospital instrument washer shown in Figure e2. Medium square-sized Ziploc polypropylene boxes were used to moderate humidity in each box, of a sufficient size to hold one N95 FFR. Both plots include data from a single run but in duplicate containers placed in different locations within the washer. Each container included a full-sized 3M 1860.

eTable 3. Dosage of pulsed xenon UV system at 1.8 meter distance from light source per 10 nm wavelength interval.

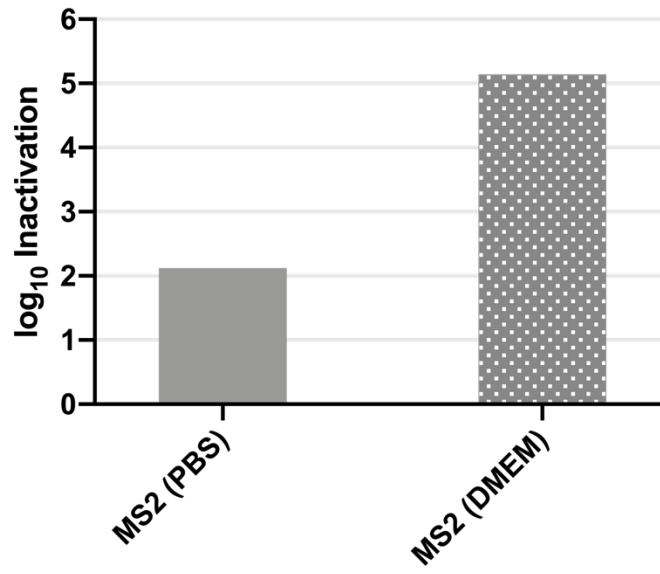
Wavelength (nm)	$\mu\text{W}/\text{cm}^2$
200-210	6.90
210-220	3.82
220-230	9.63
230-240	10.78
240-250	15.31
250-260	9.58
260-270	13.22
270-280	10.72

eTable 4. Composition of DMEM media used for droplet deposition.

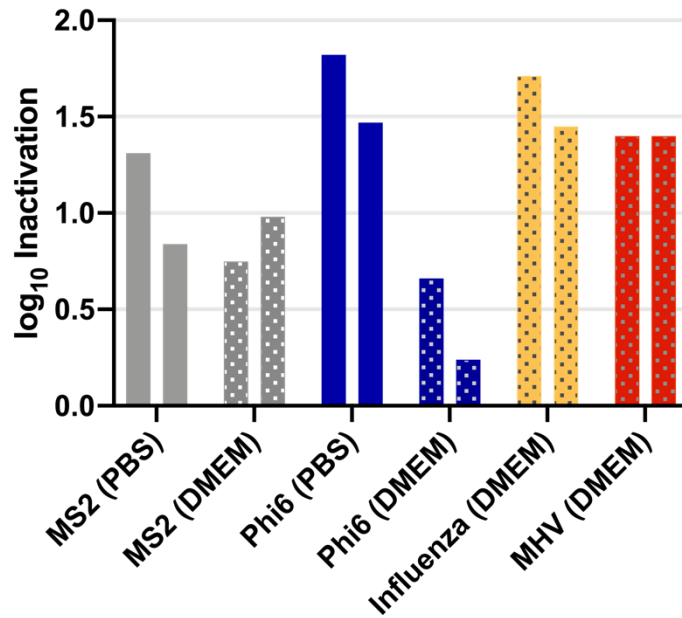
Component	Type	Concentration (mM)
<i>DMEM</i>		
Glycine	Amino Acid	0.4 mM
L-Arginine hydrochloride	Amino Acid	0.4 mM
L-Cystine 2HCl	Amino Acid	0.2 mM
L-Glutamine	Amino Acid	4 mM
L-Histidine hydrochloride-H ₂ O	Amino Acid	0.2 mM
L-Isoleucine	Amino Acid	0.8 mM
L-Leucine	Amino Acid	0.8 mM
L-Lysine hydrochloride	Amino Acid	0.8 mM
L-Methionine	Amino Acid	0.2 mM
L-Phenylalanine	Amino Acid	0.4 mM
L-Serine	Amino Acid	0.4 mM
L-Threonine	Amino Acid	0.8 mM
L-Tryptophan	Amino Acid	0.08 mM
L-Tyrosine disodium salt dihydrate	Amino Acid	0.4 mM
L-Valine	Amino Acid	0.8 mM
Choline chloride	Vitamin	0.03 mM
D-Calcium pantothenate	Vitamin	0.01 mM
Folic acid	Vitamin	0.01 mM
i-Inositol	Vitamin	0.04 mM
Niacinamide	Vitamin	0.03 mM
Pyridoxine hydrochloride	Vitamin	0.02 mM
Riboflavin	Vitamin	0.001 mM
Thiamine hydrochloride	Vitamin	0.01 mM
Calcium Chloride (CaCl ₂) (anhyd.)	Inorganic Salt	1.8 mM
Ferric Nitrate (Fe(NO ₃) ₃ ·9H ₂ O)	Inorganic Salt	0.0002 mM
Magnesium Sulfate (MgSO ₄) (anhyd.)	Inorganic Salt	0.81 mM
Potassium Chloride (KCl)	Inorganic Salt	5.33 mM
Sodium Bicarbonate (NaHCO ₃)	Inorganic Salt	44.05 mM
Sodium Chloride (NaCl)	Inorganic Salt	110.34 mM
Sodium Phosphate monobasic (NaH ₂ PO ₄ ·)	Inorganic Salt	0.91 mM
D-Glucose (Dextrose)	Other	25 mM
Phenol red	Other	0.04 mM
<i>HEPES (N-2-hydroxyethylpiperazine-N-2-ethane sulfonic acid)</i>	Organic chemical	25 mM
<i>Bovine serum albumin (Fraction V)</i>	Protein	0.1875%
<i>Penicillin/Streptomycin</i>	Antibiotics	1%

eTable 5. Composition of PBS

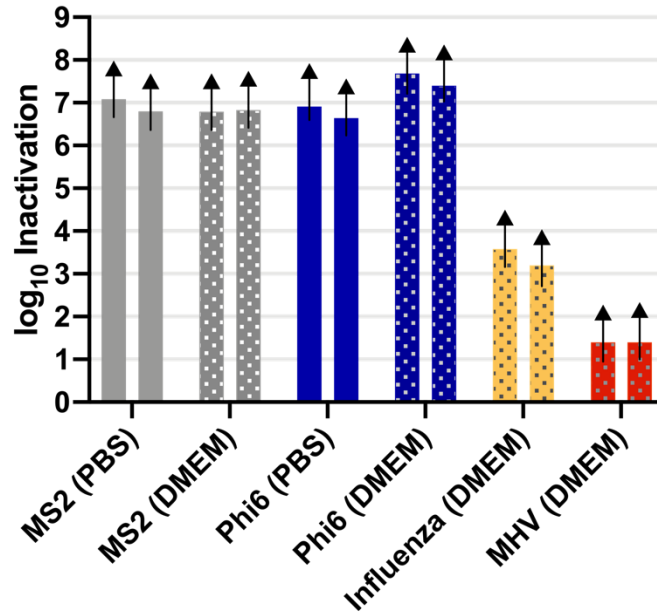
Component	Type	Concentration (mM)
Potassium Chloride (KCl)	Inorganic Salt	2.7
Potassium Phosphate (NaH ₂ PO ₄)	Inorganic Salt	1.8
Sodium Chloride (NaCl)	Inorganic Salt	137
Sodium Phosphate (NaH ₂ PO ₄)	Inorganic Salt	10



eFigure 5. MS2 control experiment with pulsed xenon UV treatment + heat with low humidity. Virus deposited in PBS or DMEM (n = 1 each).



eFigure 6. MS2 experiment with pulsed xenon UV treatment.

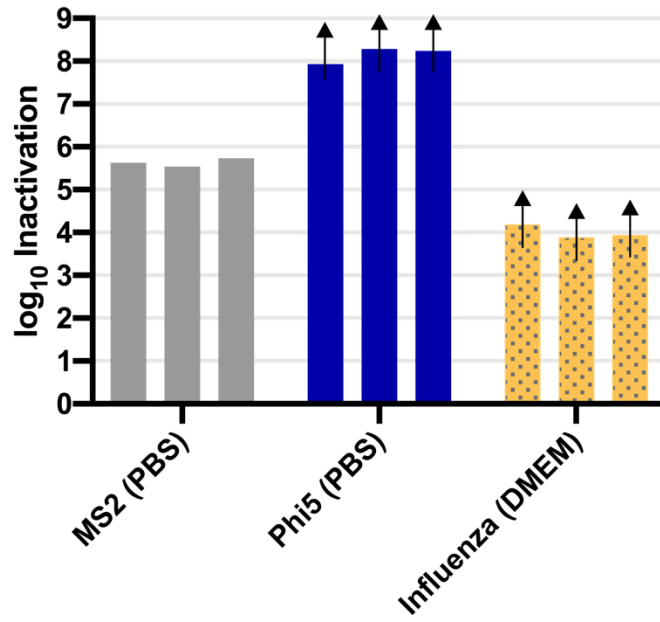


eFigure 7. Virus removal with moderate relative humidity and heat up to 80 °C for 15 minutes. Experiments were conducted on duplicate mask coupons on the same day.

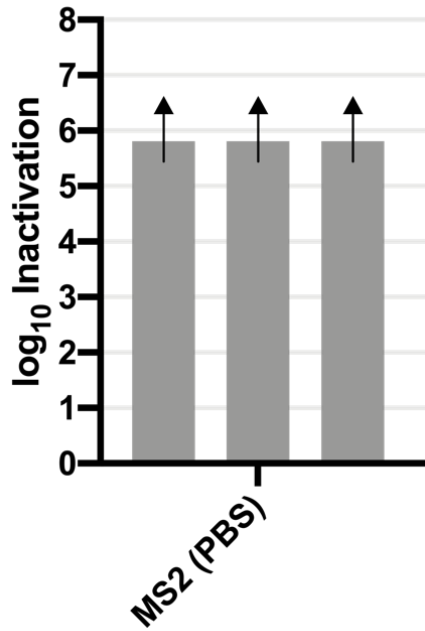
eTable 6. Log reduction values for bacterial and fungus indicators. nt = not tested

Treatment ^a	<i>S. aureus</i>	<i>E. coli</i>	<i>G. stearothermophilus</i>	<i>A. niger</i>	<i>Geobacillus</i> tablet
VHP #1 (short) ^a	1.0	>3.8	>1.4	>1.2	negative
VHP #2 ^a	>2.3	>3.8	>3.0	>3.8	negative
VHP #3 ^a	>1.6	nt	>1.8	nt	negative
UV-PX ^b	<1.0	Pending	0.06	Pending	positive
Dry heat ^b	<1.0	Pending	0.11	Pending	positive
Moderate RH + heat ^b	>2.9	Pending	0.17	Pending	positive
UV-PX + dry heat ^b	<1.2	Pending	0.06	Pending	positive
UV-PX + moderate RH + heat ^b	>2.7	Pending	0.24	Pending	positive

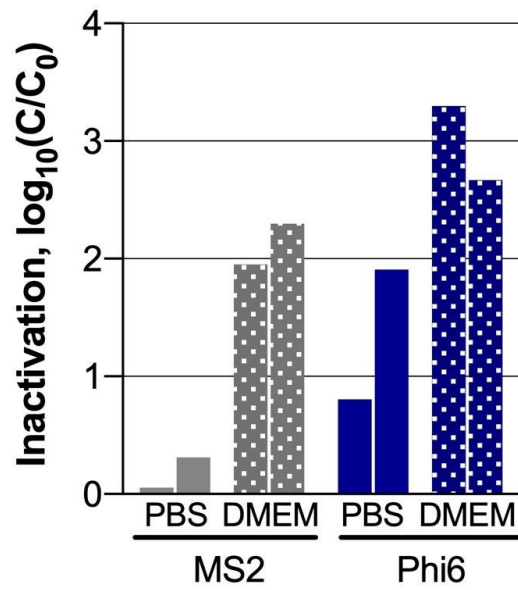
^aVHP = vaporous hydrogen peroxide; UV-PX = pulsed xenon UV; heat conditions are as defined in the main document; nt = not tested. ^arespirator coupons spiked on both front and back; ^brespirator coupons only spiked on front.



eFigure 8. Virus removal with Sterrad HPGP. Plot shows triplicate samples for each virus measured on the same day.



eFigure 9. MS2 removal with ethylene oxide. Plot shows triplicate samples for MS2 virus measured on the same day.



eFigure 10. MS2 experiment in controlled laboratory setting with heat (82 °C) with 10% RH (low humidity) and virus deposited in PBS or DMEM (n = 2 each).

References

1. Bahloul A., Mahdavi A., Haghghat F., and Ostiguy C. Evaluation of N95 filtering facepiece respirator efficiency with cyclic and constant flows. *J Occup Environ Hyg.* 2014;11(8):499-508. doi: 10.1080/15459624.2013.877590